2011 WJTA-IMCA Conference and Expo
September 19-21, 2011 ● Houston, Texas

Paper

DETERMINATION OF SPATIAL VELOCITY DISTRIBUTIONS OF ABRASIVE PARTICLES IN ABRASIVE WATER JETS USING LASER-INDUCED FLUORESCENCE UNDER REAL CONDITIONS

R. Balz, K.C. Heiniger
University of Applied Sciences Northwestern Switzerland
Windisch, Switzerland

ABSTRACT

A method is presented to determine the position and velocity of abrasive particles within high-energy abrasive water jets at positions downstream of the exit of focusing tubes. An advanced optical setup, adapted from stereo particle-image-velocimetry by using stereoscopically arranged cameras, is used to obtain full spatial resolution of fluorescent dyed abrasive particles within the three-phase flow of a high-energy abrasive water jet. The use of cameras, able to take double exposures separated by 1 μs, allows particle tracking by application of an image processing algorithm. The abrasive water jet parameters are set to correspond to real conditions in today's abrasive water jet cutting industry. Benefits of the knowledge of the spatial distributions of the abrasive particles and their velocities lie in its importance as input data for erosion models of high-energy abrasive water jet interaction with different ductile and brittle materials and in the availability of experimental data for validating computational multi-phase fluid-solid flow models of the high-energy abrasive water jet formation process. Up to now, no experimental data has been available for such distributions under real conditions.

1 INTRODUCTION

The high-energy abrasive water jet (AWJ), based on the injection method as used for most industrial cutting applications, is a complex three-phase flow with the two compressible fluids, air and water, and non-spherical, abrasive particles. Detecting single abrasive particles with velocities of several hundred meters per second and sizes of about a tenth of a millimeter in an AWJ is difficult to achieve, since under real conditions the abrasive particles are applied at frequencies in the range of hundreds of kilohertz and are surrounded by water droplets with different density; this makes it almost impossible to detect single abrasive particles mechanically with today's acoustic emission- and acceleration sensors.
Since almost all abrasion on brittle and ductile materials is caused by the accelerated abrasive particles, having exact experimental data with statistical velocities and density distributions of the abrasive particles is essential to understand and validate models of the abrasion process and computational multi-phase fluid dynamics simulations. Previous work, as [1] - [12], has shown methods to achieve detecting single abrasive particles in an AWJ, but until now no three-dimensional spatial resolution of abrasive particles has been measured or analyzed under real conditions.
The new optical measurement technique called three-dimensional laser-induced fluorescence (3D LIF) allows detecting fluorescent dyed abrasive particles downstream the exit of the focusing tube in all three spatial dimensions within the AWJ with high spatial accuracy. Since 3D LIF is an optical and therefore nonintrusive measurement technique, all conditions of the AWJ are kept unchanged and measurements can be taken under real conditions as usual in the AWJ cutting industry. The only modification in the AWJ process is the dyed abrasive particles, which are coated with a thin layer of a fluorescent dye called Rhodamine B. The dyed abrasive particles do not show any significant change in the abrasion performance compared to non-dyed, original abrasive particles.

2 EXPERIMENT

2.1 Experimental setup

A commercially available AWJ injection system with a high-pressure intensifier water-pump has been used to generate the high-energy fluid-jet. The abrasive particles have been regulated and fed to the cutting head by an abrasive dosing system using a motor driven belt. The test-rig used has been completely equipped with measurement instrumentation to guarantee optimal accuracy and repeatability. A water pressure sensor has been mounted behind a high-pressure water filter directly in front of the cutting head. The air mass-flow has been measured by a coriolis flow meter and the abrasive mass-flow by an inductive sensor in combination with a spring hanger similar to the abrasive flow rate sensor presented in [13]. The water mass-flow has been analyzed by evaluating the water pressure signal and the discharge coefficients. The orifice diameters of the nozzles used have been measured before and after the experiments to guarantee constant conditions during the optical measurements. The high-pressure intensifier water-pump allows for a pressure adjustable in the range from 50 to 400 MPa. The cutting head is equipped with a sapphire orifice of diameter 0.28 mm, and a focusing tube of diameter 0.80 mm and length 76 mm. The dyed abrasive particles are mesh 120 Garnet, cleaned with water to reduce noise

(caused by loose dye pieces) in the images and sized after the coating process to minimize deviations from original abrasive particles.
The whole cutting head can be moved along the focusing tube axis (which is to define the z-direction) to adjust the stand-off distance between the end of the focusing tube (corresponding to $z = 0$) and the measurement volume field of view (FOV). A catcher has been used to dissipate the AWJ's energy and collect the slightly toxic and ecologically damaging Rhodamine B contaminated water and used abrasive particles. The catcher also allowed removing dense fog around the AWJ by suction using a vacuum to increase the probability of laser light to enter the AWJ's core.

2.2 Laser-induced fluorescence

The functionality of the laser-induced fluorescence (LIF) method is described in more detail in [1]. The basic principle is that a fluorescent dye can absorb a certain wavelength spectrum and emit light at a shifted, characteristic wavelength immediately. In this case, the emitted light has lower energy and therefore a higher wavelength. The fluorescent dye Rhodamine B ($C_{28}H_{31}ClN_2O_3$, CAS number 81-88-9) has been used for its good quantum and application properties. The abrasive particles are coated with a thin layer of Rhodamine B, so that the change in density is insignificant. A double pulse Nd:YAG laser with second harmonic generation, which emits at 532 nm, is used to excite the fluorescent dye. The use of high-pass filters allows the two CCD cameras to capture only light emitted by the dyed abrasive particles, but not reflections and refractions from the laser light on the free surfaces in the three-phase flow.

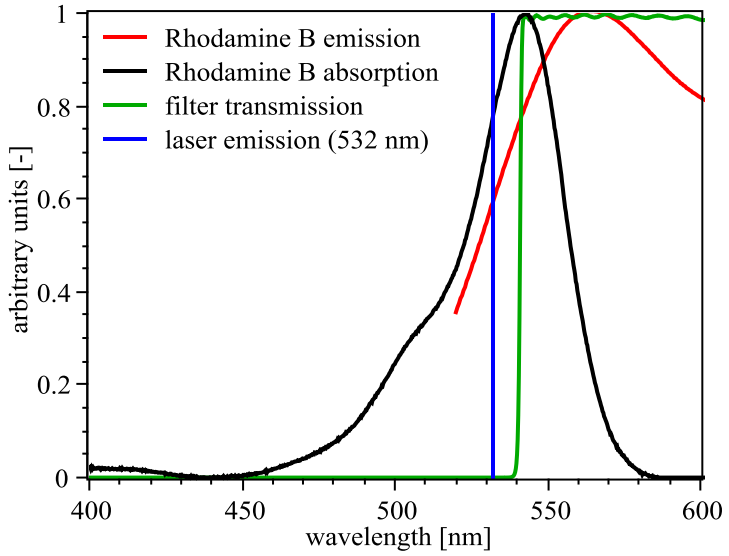

Figure 1. Fluorescence spectrum of Rhodamine B

Figure 1 shows emission and absorption spectra of the fluorescence dye Rhodamine B (data from [14]), the laser emission at 532 nm and the transmission of the optical high-pass filter.

2.3 Optical setup

The key components are the double pulse Nd:YAG laser with an energy of 120 mJ and a pulse width of 5 ns, the two fast frame-transfer CCD cameras and the corresponding long-distance microscope and zoom lens.

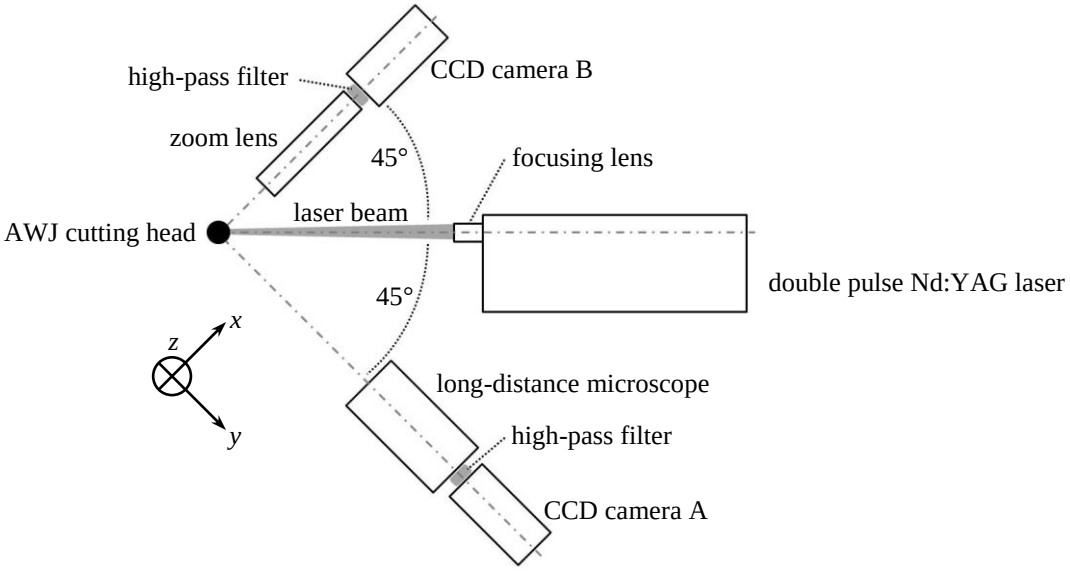

Figure 2. Top view of optical setup and alignment of cameras and laser

To get the velocity information of the fluorescent dyed abrasive particles, double frame images, which are separated by a delay of 1 μs, had to be taken to guarantee minimal displacement of the abrasive particles. By evaluating the particles position in both frames, a distance can be calculated and from this a particle velocity is deduced. The abrasive particles in the images are not smeared out since the laser pulse and therefore the exposure is only 5 ns long. The optical setup has been optimized from the previous work with LIF (see [1] for further information).

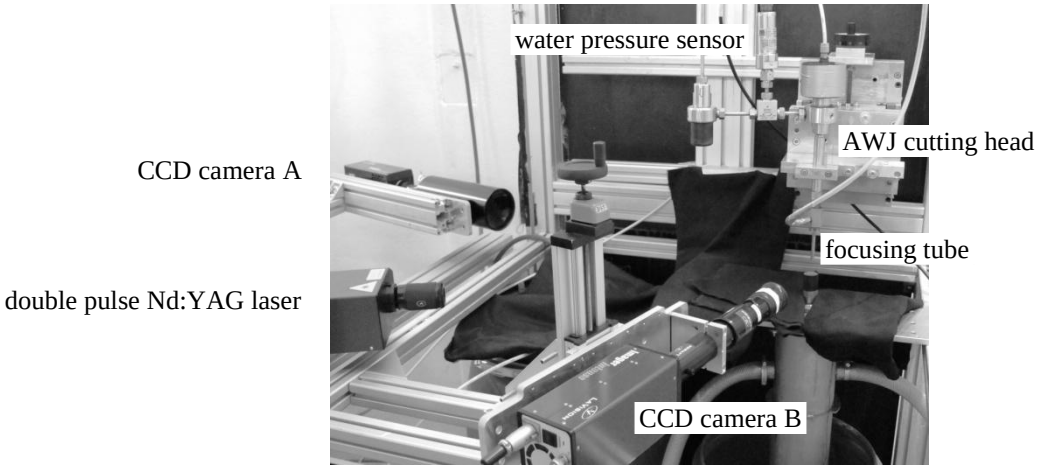

Figure 3. Experimental setup

The high-pass filter has been replaced by a high-pass edge function filter with higher optical density at the laser wavelength, higher transmission for wavelengths of interest and sharper edge to achieve better optical performance with an increased contrast between particles and background noise.
The laser beam is focused, its diameter reduced to get a maximal number of photons into the AWJ. A longer distance between the long-distance microscope and the AWJ increased the depth of field. These improvements yielded better images and therefore reduced the effort in image evaluation, so that the acquired data only needed a minimal visual inspection after the image processing. The image evaluation has been fully automated, what allows for analyzing much more data for more accurate statistical results.

2.4 Image processing

The image processing is based on a method presented in [1]. This method is modified for the new high-pass filters and the stereoscopic information. The double images from CCD camera A are used to determine position and velocity of the abrasive particles, since the long-distance microscope provides a depth of field bigger than the AWJ diameter, thus all particles detected appear sharp on the images by camera A. CCD camera B in turn, equipped with a zoom lens, which has a depth of field only a fraction amount of the AWJ diameter, is used to determine the position of the particle to get the spatial information. Since both cameras deliver similar information, the acquired data has been cross-checked with respect to the velocity components and particle positions.

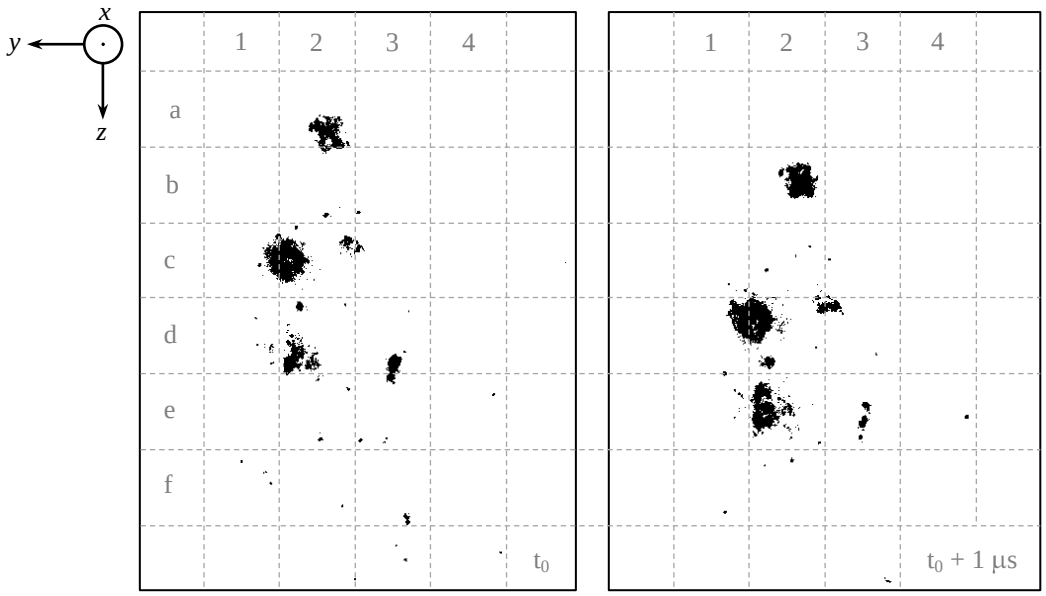

Figure 4. Acquired images of CCD camera B. Frame 1 (left) and Frame 2

Figure 4 shows Frame 1 and Frame 2 of the CCD camera B with the corresponding coordinate system which indicates the AWJ flow direction *z*. The frames shown are taken with a delay of 1 µs, they are inverted in terms of gray scales, and the gray-level histogram has been adjusted for better image contrast. Reflections of laser-light on the water jet are not visible at all, since the high-pass filter blocks this wavelength almost completely. The field of view (FOV) is

2.52 mm x 3.34 mm with a resolution of 1040 x 1376 pixels. The water pressure during the optical measurement was 103.2 ± 2.3 MPa and the abrasive mass flow 0.115 ± 0.006 kg/min.
Since more than one abrasive particle can be detected in the FOV with this new optical setup, a particle identification algorithm had to be written to identify different abrasive particles and their positions. The algorithm also separates signals from abrasive particle splitters and dropped-off dye, by evaluating shape and size of the detected particles.
The developed algorithm detects three abrasive particles in each of both frames in Figure 4, together with their individual positions and velocities. The detected abrasive particles in Frame 1 are located at the positions a2, c2 and d2 in Figure 4. In addition, the exact three dimensional positions of the abrasive particles can be determined with the two frames of the stereoscopically arranged second camera (CCD camera A). There is a minor quantity of about 10 to 15 % of all detected abrasive particles that are not found on the frames of the second camera. This data is neglected for further analysis.

3 RESULTS

3.1 Definitions

The results are presented in terms of dimensionless numbers. The abrasive particles velocity is scaled by the water velocity after the orifice neglecting the friction and compressibility of the water.

$$V = \frac{v_P}{\sqrt{2 \cdot \Delta p_W / \rho_W}} \tag{1}$$

A dimensionless radial position is defined as the ratio between the dimensional radial position of abrasive particles and the focusing tube radius,

$$R = r_P / r_F \tag{2}$$

a dimensionless stand-off distance is defined as the ratio between the axial distance downstream the exit of the focusing tube and the focusing tube inner diameter

$$Z = z / d_F \tag{3}$$

and a dimensionless mass flow ratio is defined as the ratio between the mass flow of abrasive particles and the mass flow of the water jet.

$$M = \dot{m}_P / \dot{m}_W \tag{4}$$

3.2 Abrasive particle distribution

Figure 5 shows the positions of 4777 abrasive particles detected between the stand-off distances Z=1.25 and Z=5, projected to a single plane. The plotted circle indicates the focusing tube inner diameter d_F and the filled black circle in the right bottom corner of the graph indicates the medium size of the used mesh 120 Garnet abrasive particles. Positions of detected abrasive particles can be evaluated in three dimensions; the scatterplot in Figure 5 shows that indeed abrasive particles can be detected at any position within the AWJ downstream the exit of the focusing tube. However a noticeable higher concentration of abrasive particles in the upper-left area indicates the 45° direction of the focused incident laser beam. The free surfaces of water droplets and air bubbles in the AWJ reduce the probability of the incident light beam to illuminate abrasive particles in the rear part of the AWJ, and in turn the light emitted by the corresponding abrasive particles is reduced because of occurring reflections and refractions.
Figure 6 shows an abrasive particle distribution between Z=1.25 and Z=5. The data has been fitted to a Gaussian curve, and the two vertical lines indicate the focusing tube walls.

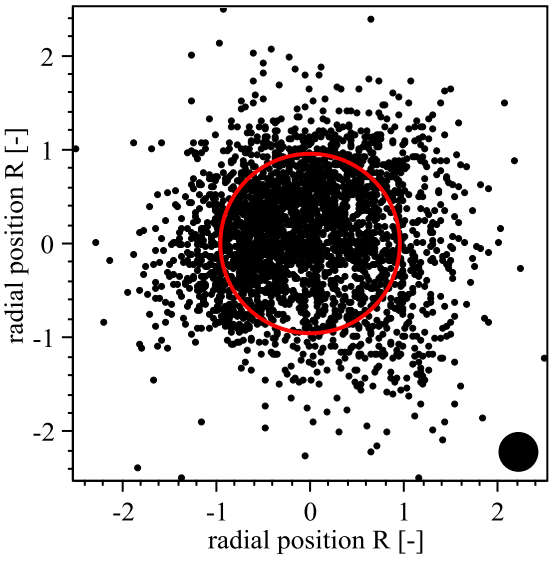

Figure 5. Scatterplot of abrasive particles

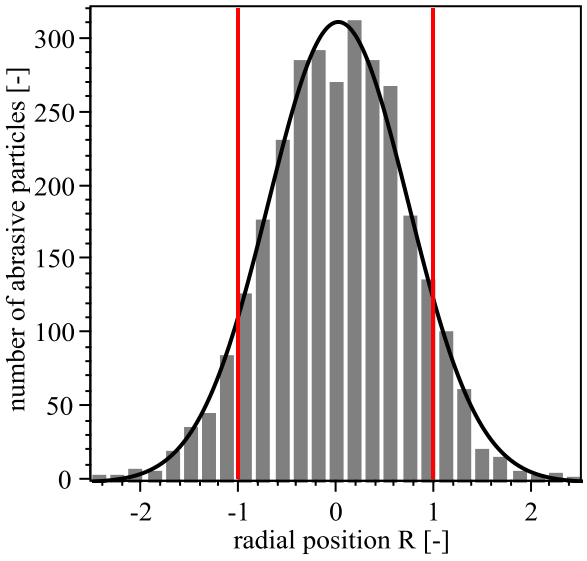

Figure 6. Histogram of abrasive particles

The histogram shows that the abrasive particles can be considered symmetrically distributed with the maximum near the focusing tube axis at the radial position R=0. The AWJ parameters for the data shown are the same as mentioned in section 2.4.

3.3 Abrasive particle velocity distribution

Figure 7 shows axial velocity distributions of abrasive particles between Z=1.25 and Z=5 with different water pressures. The axial velocities of the abrasive particles have been averaged in spatial bins and the standard deviations are plotted as error bars. The axial velocity distributions of the abrasive particles are almost constant within the focusing tube diameter. The mass ratio for all evaluated axial velocities is M=0.1. The plots in Figure 7 are limited in radial position at the focusing tube walls, since only about 4000 abrasive particles have been detected per AWJ parameter. With this amount, only a few hundred abrasive particles are detected outside the

focusing tube diameter, since most of the abrasive particles at this stand-off distances lie in the core of the AWJ, as indicated in Figure 6.

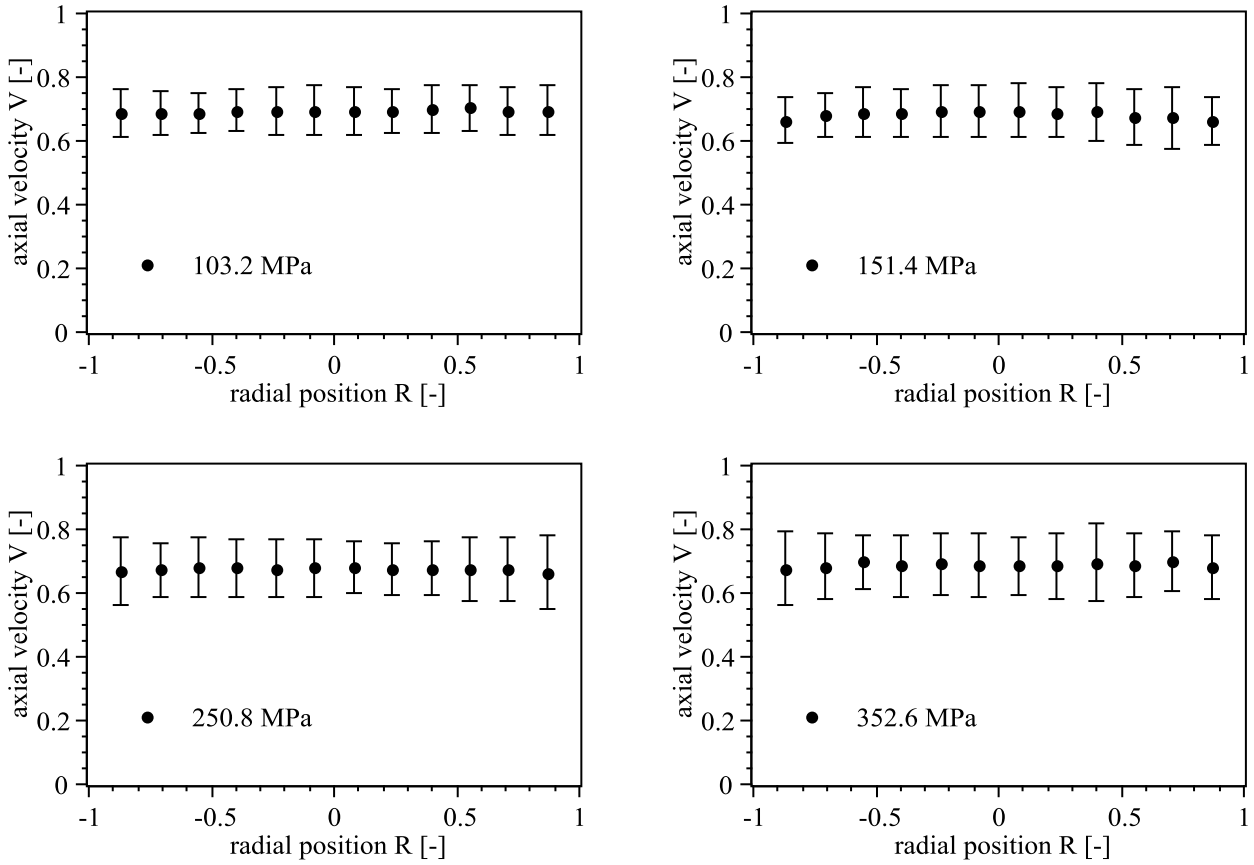

Figure 7. Axial velocity distributions of abrasive particles for different water pressures

Since the optical system is limited regarding the frame rate, images can be taken with 5 Hz and therefore, theoretically, only about 1/100'000 of all abrasive particles can be detected during an experiment. This is due to the continuously running AWJ, the relatively low data transfer rates of the cameras and the charging time of the double pulse Nd:YAG laser, in comparison to times related to the speed of the abrasive particles.

4 CONCLUSIONS

The acquired and evaluated data shows that the 3D LIF measurement technique allows detecting fluorescent dyed abrasive particles within an AWJ under real conditions. The taken images indicate that the abrasive particles are not single events; they are agglomerated in the AWJ.
The experimental data provides the following results for a mass flow ratio M=0.1 and the used focusing tube, orifice and mesh size:

- The distribution of abrasive particles within an AWJ based on the injection method is approximately Gaussian and symmetrical to the focusing tube axis.

- The velocity distribution downstream the exit of the focusing tube is almost flat, i.e. the axial velocity virtually independent of the radial position, with slightly slower abrasive particles near the focusing tube walls.

5 ACKNOWLEDGEMENTS

This work has been funded by the European Commission's 7th Framework Program as part of the project ConforM-Jet (grant agreement no. 229155). The authors would like to acknowledge the many valuable suggestions made by Chidambaram Narayanan and Daniel Weiss as well as the support from Herbert Looser and Patrick Coray regarding the optical measurement technique.

6 REFERENCES

[1] P. Roth, H. Looser, K. C. Heiniger, S. Bühler, "Determination of abrasive particle velocity using laser-induced fluorescence and particle tracking methods in abrasive water jets", Proceedings of 13th American Waterjet Conference, 2005, Houston, Texas

[2] R. K. Swanson, M. Kilman, S. Cerwin, W. Carver, "Study of particle velocities in water driven abrasive jet cutting", Proceedings of 4th U.S. Waterjet Conference, 1987, Berkeley, California

[3] A. L. Miller, J. H. Archibald, "Measurement of particle velocities in an abrasive jet cutting system", Proceedings of 6th American Waterjet Conference, 1991, Houston, Texas

[4] U. Himmelreich, W. Riess, "Laser-velocimetry investigations of the flow in abrasive water jets with varying cutting head geometry", Proceedings of 6th American Waterjet Conference, 1991, Houston, Texas

[5] H.-T. Liu, P. J. Miles, N. Cooksey, C. Hibbard, "Measurements of water-droplet and abrasive speeds in a ultrahigh-pressure abrasive-waterjets", Proceedings of 10th American Waterjet Conference, 1999, Houston, Texas

[6] A. Dorle, L. J. Tyler, D. A. Summers, "Measurements of particle velocities in high speed waterjet technology", Proceedings of 12th American Waterjet Conference, 2003, Houston, Texas

[7] W.-L. Chen, E. S. Geskin, "Measurement of the velocity of abrasive waterjet by the use of laser transit anemometer", Proceedings of 10th International Conference on Jet Cutting Technology, BHR Group, 1990, Amsterdam, Netherlands

[8] K. F. Neusen, T. J. Gores, T. J. Labus, "Measurement of particle and drop velocities in a mixed abrasive waterjet using a forward-scatter LDV system", Proceedings of 11th International Conference on Jet Cutting Technology, BHR Group, 1992, St. Andrews, Scotland

[9] K. F. Neusen, D. G. Alberts, T. J. Gores, T.J. Labus, "Distribution of mass in a three-phase abrasive waterjet using scanning x-ray densitometry", Proceedings of 10th International Symposium on Jet Cutting Technology, BHR Group, 1990, Amsterdam, Netherlands

[10] T. Sawamura, Y. Fukunishi, R. Kobayashi, "Study of the abrasive waterjet structure by measuring water and abrasive particle velocities separately", Proceedings of 14th International Conference on Jetting Technology, BHR Group, 1998, Brugge, Belgium

[11] X. Claude, A. Merlen, B. Thery, O. Gatti, "Abrasive waterjet velocity measurements", Proceedings of 14th International Conference on Jetting Technology, BHR Group, 1998, Brugge, Belgium
[12] Y. Dong, L. J. Tyler, D. A. Summers, M. Johnson, "Experimental study of particle velocity measurement in abrasive water jet cutting in the nozzle and jet stream using multiple sensing elements", Proceedings of 17th International Conference on Water Jetting, BHR Group, 2004, Mainz, Germany
[13] M. Hashish, D. O. Monserud, P. D. Bondurant, J. C. Hake, S. J. Craigen, G. B. White, W. J. Coleman, "A new abrasive-waterjet nozzle for automated and intelligent machining", Proceedings of 7th American Waterjet Conference, 1993, Seattle, Washington
[14] http://omlc.ogi.edu/spectra/PhotochemCAD/html/rhodamineB.html, status 02.03.2011

7 NOMENCLATURE

p_w	[Pa]	water pressure
ρ_w	[kg/m^3]	water density
v_P	[m/s]	abrasive particle velocity
V	[-]	dimensionless number for abrasive particle velocity
r_P	[m]	abrasive particle radial position
R	[-]	dimensionless number for abrasive particle radial position
z	[m]	axial distance from exit of focusing tube
d_F	[m]	inside diameter of focusing tube
r_F	[m]	inside radius of focusing tube
Z	[-]	dimensionless number for axial position after exit of focusing tube
t_0	[s]	point in time
$\dot{m}_P$	[kg/s]	mass flow of abrasive particles
$\dot{m}_W$	[kg/s]	mass flow of water jet
M	[-]	dimensionless number for mass flow ratio between abrasive particles and water jet